Silicon isotopes: from cosmos to benthos

Ramananda Chakrabarti*

Centre for Earth Sciences, Indian Institute of Science, Bengaluru 560 012, India

Silicon is the second most abundant element on the Earth and one of the more abundant elements in our Solar System. Variations in the relative abundance of the stable isotopes of Si (Si isotope fractionation) in different natural reservoirs, both terrestrial (surface and deep Earth) as well as extra-terrestrial (e.g. meteorites, lunar samples), are a powerful tracer of present and past processes involving abiotic as well as biotic systems. The versatility of the Si isotope tracer is reflected in its wide-ranging applications from understanding the origin of early Solar System objects, planetary differentiation, Moon formation, mantle melting and magma differentiation on the Earth, ancient sea-water composition, to modern-day weathering, clay formation and biological fractionation on land as well as in the oceans. The application of Si isotopes as tracers of natural processes started over six decades ago and its usage has seen a sudden increase over the last decade due to improvements in mass spectrometry, particularly the advent of multi-collector inductively coupled plasma mass spectrometers, which has made Si isotope measurements safe and relatively easy while simultaneously improving the accuracy and precision of measurements.

Keywords: Mass spectrometry, meteorites, sea water, silicon isotopes, weathering.

ISOTOPE geochemistry is a discipline that utilizes variations in the relative abundance of isotopes of elements as tracers of natural processes. Although there are almost 60 naturally occurring elements that are not radioactive or have a very long half life (~ one billion years or more and hence essentially stable) and have more than one isotope, traditional stable isotope geochemistry studies have typically focused on the elements H, O, C, N and S. Traditional stable isotope geochemistry has been successfully applied to diverse problems, including the origin and evolution of our Solar System, crust and mantle evolution, origin of life, palaeoclimate reconstruction, and modern climate studies amongst many others. Breakthroughs in Earth and planetary science, especially in geochemistry, follow the development of instrumentation which provides newer and more precise analytical data on natural materials. The evolution of the field of 'non-traditional', stable isotope geochemistry in the last ten years is a direct result of the advent of multi-collector inductively coupled plasma mass spectrometry (MC-ICPMS; c.f. refs 1 and 2).

Silicon (Si) is one of the most abundant elements on the Earth as well as the Solar System and has three stable isotopes with masses 28, 29 and 30. The earliest studies involving Si isotope ratio measurements date back to the early 1950s (e.g. Reynolds and Verhoogen[3]). These measurements were done using gas-source isotope ratio mass spectrometers (IRMS), which involved the use of very hazardous gases such as F_2 or BrF_5. The complexity of these measurements resulted in limited use of Si isotopes as a 'tracer' of terrestrial and planetary processes. The first MC-ICPMS Si isotope data were reported in 2002 by De La Rocha[4]; this new measurement tool eliminated the use of hazardous reagents and has propelled the use of Si isotopes in geochemical and cosmochemical research. Over 40 papers on Si isotope ratio measurements in a variety of natural objects using MC-ICPMS have been published since 2002. Being a widely abundant element in nature, Si isotope fractionation has been documented for a wide variety of natural processes as diverse as planetary differentiation to secretion of siliceous shells by microorganisms. Here, I present an overview of the application of Si isotopes in tracing processes from early Solar System evolution (cosmos) to biological fractionation in the marine environment (benthos).

Measurement techniques

Since 2002, most published Si isotope ratio measurements are using a MC-ICPMS. However, the use of IRMS for Si isotope ratio measurements continues with recent modifications involving conversion of silica to Cs_2SiF_6 followed by acid reaction to produce SiF_4 gas[5], laser heating of precipitated silica[6], etc. Prior to MC-ICPMS measurements, samples have to be dissolved and purified. The traditional method of using hydrofluoric acid (HF) for dissolving silicate samples can potentially fractionate Si isotopes due to the volatile loss of SiF_4, which forms during this dissolution process. It has been argued that limited use of HF does not fractionate Si isotopes[4,7–9]. However, mass bias instability during mass spectrometry can occur[10]. Hence, samples are fused using an alkali flux followed by dissolution in dilute inorganic acids and separation of Si from the sample matrix using ion-exchange chromatography (e.g. refs 10–13). Ion-exchange chromatography eliminates interferences from doubly charged species like $^{56}Fe^{2+}$, $^{58}Fe^{2+}$ and $^{58}Ni^{2+}$, and

*e-mail: ramananda@ceas.iisc.ernet.in

$^{60}Ni^{2+}$ on masses 28, 29 and 30 respectively, during mass spectrometry as well as reduces the matrix effect which can affect isotopic measurements (e.g. ref. 14). However, molecular species which are generated in the plasma and cause isobaric interferences (e.g. $^{14}N_2^+$ and $^{12}C^{16}O^+$ for mass 28, $^{14}N_2H^+$ for mass 29 and $^{14}N^{16}O^+$ for mass 30) have to be resolved. This is typically done by analyses in medium or high resolution (cf. ref. 15) as well as the use of H_2 and He in small amounts in a collision cell, if this option is available in the MC-ICPMS (cf. ref. 11). Analyses in high resolution, however, reduces sensitivity. Hence Si concentration in samples and standards, matched to within 10%, have to be between 1 and 5 ppm for acceptable counting statistics.

Since Si has only three stable isotopes, it is not possible to use the more definitive double-spiking technique[16] for accurate determination of Si isotope fractionation in nature. To correct for instrumental mass fractionation, a sample-standard bracketing technique has to be used. This technique assumes that the mass bias of the sample and the bracketing standard are similar. Early IRMS Si isotope ratio measurements used Cal Tech Rose Quartz as the bracketing standard[17–24]. The first Si isotopic study to use the NBS28 standard was done by Molini-Velsko *et al.*[25]. For MC-ICPMS measurements, the NBS28 standard is also chemically processed in the same way as the sample, prior to analysis. Delta values are calculated as $\delta^{xx}Si(‰) = [(^{xx}Si/^{28}Si)_{sample}/(^{xx}Si/^{28}Si)_{NBS28}) - 1] \times 1000$ (permil, ‰), where *xx* is either mass 29 or 30. After successful chemistry and mass spectrometry, all samples and standards analysed should plot on a mass-dependent fractionation line in a three-isotope plot with a slope close to one-half. An alternate method to correct for instrument fractionation during Si isotope ratio measurements is to simultaneously measure Mg-isotopes in Mg-doped samples and standards[7,26] assuming that the instrument fractionation of Mg and Si isotopes is similar. Several inter-laboratory standards like Diatomite, Big Batch, IRMM018, NBS28, Harvard-AA and Harvard-HPS[11,27–29] have been prepared and calibrated. These standards are also chemically processed and routinely measured along with unknown samples to test for accuracy of measurements. With improved instrumentation, sub-0.1‰ data for $\delta^{30}Si$ can now be obtained routinely using MC-ICPMS.

In situ measurements of Si isotopes using MC-ICPMS involve ablation of the sample by lasers prior to introduction in the plasma for ionization; high-precision data have been reported using LA-MC-ICPMS[30–32]. *In situ* Si isotope data can also be obtained using MC-SIMS (secondary ion mass spectrometry). While this technique allows sampling in high spatial resolution, it is limited to a 2σ uncertainty of 0.3‰ for $\delta^{30}Si$ (ref. 33), which although a significant improvement compared to earlier ion-probe studies (e.g. refs 34–37), is still three times less precise than MC-ICPMS.

Si isotopes in bulk meteorites and their components

In the early studies of bulk meteorites, a $\delta^{30}Si$ range of 2‰ was observed in the different meteorite groups derived from both primitive as well as differentiated planetesimals and no resolvable difference was observed between the average $\delta^{30}Si$ in terrestrial igneous rocks, meteorites and lunar samples. Bulk meteorites showed mass-dependent silicon isotope fractionation and isotopic anomalies were not observed (cf. ref. 25). In contrast, larger (3–4‰) fractionation in $\delta^{30}Si$ has been observed in many refractory inclusions of chondritic meteorites[38–40] (Figure 1). These large variations in $\delta^{30}Si$ have been explained by isotopic exchange reactions between nebular-SiO gas and silicate condensates forming from it and can be modelled by a Rayleigh process[38]. Some calcium- and aluminum-rich inclusions (CAIs) from the chondritic meteorite Allende (e.g. C1, EK 1-4-1, CG-14, HAL, labelled 'FUN' – unknown nuclear fractionations) show anomalous compositions of isotopes of many elements. $\delta^{30}Si$ values of these FUN inclusions show a range of

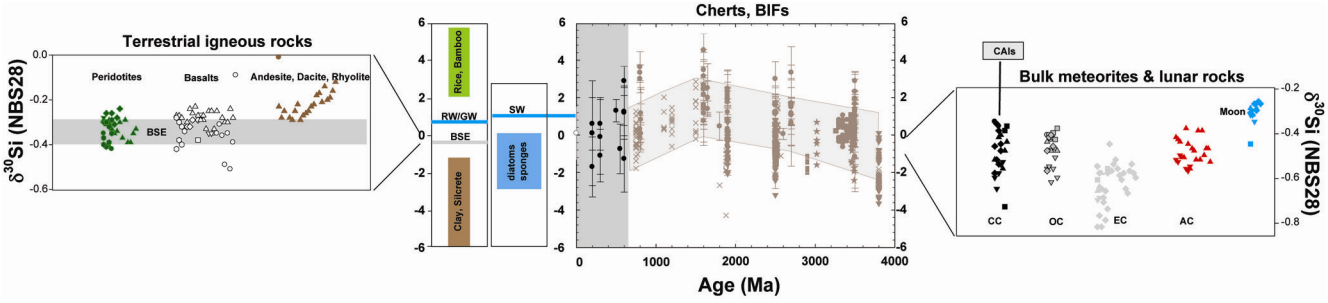

Figure 1. Schematic diagram showing Si isotope ($\delta^{30}Si$, mostly MC-ICPMS data) variability in natural material from bulk meteorites and their components (CAIs, calcium–aluminum-rich inclusions), bulk lunar rocks, terrestrial igneous rocks, and Precambrian and Phanerozoic cherts. Also shown as shaded regions are the domains of the $\delta^{30}Si$ of bulk silicate earth (BSE), river and groundwater (RW, GW), products of terrestrial weathering like clays and silcretes, land plants, average present-day sea water (SW), diatoms and sponges, etc. Large fractionations observed in 'FUN'-CAIs inclusions and pre-solar grains are not plotted.

~25‰, which is an order of magnitude higher than most other natural objects that have been measured for their Si isotopic composition (e.g. ref. 41). Largest fractionation (100s ‰) of Si isotopes are observed in pre-solar SiC grains, which are thought to have been formed in AGB stars[42,43].

The range of δ^{30}Si in bulk meteorites and terrestrial igneous rocks as measured by recent MC-ICPMS measurements (e.g. refs 11, 44) is an order of magnitude less compared to the older IRMS data for the same (e.g. ref. 25). Reported δ^{30}Si values for bulk carbonaceous and ordinary chondrites are indistinguishable (e.g. refs 11, 44, 45), although some researchers have argued for a marginally (by ~0.1‰) lighter δ^{30}Si in bulk ordinary chondrites compared to carbonaceous chondrites[46]. Enstatite chondrites, however, clearly show lighter δ^{30}Si compared to other chondrite groups[9,11,44,46,47] (Figure 1). The light Si is hosted in metals in enstatite chondrites (as well as in their differentiated counterparts, aubrites)[9,47,48]. The metal-free silicate portion of enstatite chondrites shows similar δ^{30}Si compared to other bulk chondrites[47], thereby suggesting broad homogeneity in the silicon isotopic composition of silicates condensing from the solar nebula. Non-chondritic meteorites do not show much variation in δ^{30}Si, which overlaps with that of bulk carbonaceous and ordinary chondrites[11,44–46] (Figure 1).

Bulk silicate Earth Si isotopic composition

Si isotope data for terrestrial rocks were first reported in the 1950s (ref. 3). However, the first comprehensive study of Si isotopes in terrestrial samples was reported by Douthitt[18] ~30 years later. He reported that igneous rocks show a range of 1.1‰ in δ^{30}Si, which correlated with silicon content and argued for a mean δ^{30}Si of –0.4‰ (precision of 0.3‰) for terrestrial mafic and ultramafic igneous rocks. Another decade and half later, Georg *et al.*[44] reported the first high-precision MC-ICPMS data for a wide suite of mafic and ultramafic terrestrial igneous rocks and concluded that δ^{30}Si of the bulk silicate Earth (BSE) is –0.38 ± 0.06‰. Subsequent studies have argued for similar δ^{30}Si (BSE) values ranging from –0.28 ± 0.02‰ based on peridotites and ocean-island basalt analyses[46], –0.33 ± 0.08‰ based on analyses of San Carlos olivine[9]; –0.38 ± 0.02 based on analyses of terrestrial basalts from different tectonic settings and localities, dunites as well as mantle-derived olivine and pyroxenes[11], to –0.24 ± 0.09 based on mafic and ultramafic USGS rock standards[26]. A more elaborate study of mafic and ultramafic terrestrial rocks yielded a δ^{30}Si (BSE) of –0.29 ± 0.08‰ (ref. 49), which is similar within analytical uncertainties to other studies (Figure 1).

High-temperature fractionation of Si isotopes is expected to be minimal. This is consistent with the lack of measurable Si isotopic variability in co-existing mantle minerals (e.g. Chakrabarti and Jacobsen[11]). However, δ^{30}Si of evolved bulk igneous material (andesite, dacite, rhyolite, etc.) is heavier compared to δ^{30}Si (BSE) and correlates with increasing silica content[50] (Figure 1). This observation is consistent with the original suggestion of Douthitt[18], which was based on less precise data. The calculated δ^{30}Si of average continental crust with an average SiO_2 content of 60 wt%, derived solely from magmatic differentiation of the mantle is however indistinguishable from the BSE value[50].

Core formation on Earth and the BSE–chondrite δ^{30}Si difference (or the lack of it)

It has been long known that the density of the Earth's Fe–Ni core is lighter than a pure Fe–Ni alloy[51,52], indicating the presence of elements lighter than Fe in the Earth's core[53]. Silicon is considered to be one of the probable light elements in the Earth's core[54]. If true, this should be accompanied by silicon isotope fractionation between metal (core) and silicates (mantle), as observed in aubrites and enstatite chondrites[9,47], high pressure–temperature experiments[8,55] as well as theoretical Si isotope fractionation calculations[56]. If indeed Si is partitioned into the Earth's core during differentiation, this should result in an unique Si isotopic composition of the Earth's mantle (BSE) and the extent of fractionation would depend on the fractionation factor between co-existing metal and silicate at the core–mantle boundary conditions, which are approximated by other geochemical and isotopic proxies (e.g. refs 57–60), and the extent of Si entering the core.

Early work on Si isotopes did not indicate any difference in δ^{30}Si of the BSE and chondritic meteorites[25]. This could, however, be due to larger analytical uncertainties of these measurements. Georg *et al.*[44] first suggested that δ^{30}Si of the silicate Earth is heavier by 0.2‰ relative to meteorites ($\Delta^{30}Si_{BSE-chondrite} = 0.2$). A similar argument was put forward by Fitoussi *et al.*[46], although they argued for a smaller $\Delta^{30}Si_{BSE-chondrite}$ of 0.08 ± 0.04 (1SD). In contrast, Chakrabarti and Jacobsen[11] found $\Delta^{30}Si_{BSE-chondrite}$ of 0.035 ± 0.035, which limited the amount of Si in the Earth's core to less than 3.84% and that of oxidized Fe in the mantle during the first 90% of planetary accretion to as low as ~1%. Armytage *et al.*[45] argued for a larger $\Delta^{30}Si_{BSE-chondrite}$ (excluding enstatite chondrites), which translated to 2.5–16.8 wt% Si in the Earth's core. The use of Si isotopes to estimate how much Si is present in the Earth's core depends on the Si isotopic composition of the starting material that formed the Earth, often termed the chondritic uniform reservoir (CHUR). This might not be any particular chondrite group. Based on other geochemical and isotopic proxies, the composition of enstatite chondrites is quite similar to the BSE. However, δ^{30}Si values of enstatite chondrites

do not overlap with those of terrestrial material[9,11,44,46,47]. Recent studies have suggested that a maximum of 15% enstatite chondrites together with CO and CI chondrites could approximate the CHUR value[48].

The Earth–Moon system

The silicate Earth and the Moon show considerable geochemical differences, although they show identical isotopic compositions of different elements like O, Cr, W, Ti, etc.[61–64]. In addition, it has been long considered based on numerical simulations that ~80% of the Moon is derived from the Mars-sized impactor that collided with the proto-Earth[65]. To explain the isotopic similarity of the BSE and the Moon, a large-scale isotopic equilibration of the proto-lunar disk and the Earth has been suggested[66]. Pahlevan *et al.*[67] suggested that the Moon and the BSE should have a 0.14‰ offset in δ^{30}Si for the Moon to have a Fe/Fe + Mg ratio twice that of the BSE.

Silicon isotope analyses of lunar samples and meteorites date back to almost 40 years ago (e.g. ref. 19). In contrast to the difference in δ^{30}Si between BSE and primitive meteorites, the extent of which is debated, δ^{30}Si of the average Moon is identical to that of the BSE[11,44,68]. No systematic differences exist between bulk samples of different lunar lithologies, e.g. the high-Ti and low-Ti basalts, Highland rocks and lunar glass[68] (Figure 1). The indistinguishable Si isotopic composition of the Earth and the Moon does not require any later large-scale Si isotopic equilibration in the vapour cloud[66] after the Moon-forming impact. Instead, it is consistent with recent simulations suggesting that the proto-lunar disk was derived primarily from the mantle of a fast-spinning proto-Earth after the giant impact[69].

Si isotopes in the modern Earth system

As discussed in the previous sections, Si isotope fractionation at high temperatures is limited. δ^{30}Si of the average continental crust is indistinguishable from the BSE, with estimated δ^{30}Si varying between –0.3‰ and –0.4‰. Silica sources to the oceans include continental weathering, hydrothermal fluids and seafloor weathering of basalts. Of these, continental weathering is the dominant source of silica to the oceans, delivered primarily as dissolved silicic acid (H_4SiO_4) in river water[70] as well as groundwater[71]. The flux of suspended silica-rich particles in river water is high, but long time-durations of dissolution of this particulate matter result in little contribution of silicic acid to the oceans from this source[70]. Si isotopes are fractionated during continental weathering and associated clay formation; lighter isotopes of Si are preferentially sequestered into secondary clay minerals, which consequently display lower δ^{30}Si values[72–77] (Figure 1). Based on first principles calculations, a 1.6‰ fractionation is estimated between quartz and kaolinite at ~27°C at equilibrium conditions[78]. δ^{30}Si of suspended silica in rivers is similar to average igneous rocks and shales, whereas δ^{30}Si of the dissolved load is higher (~+0.8; Figure 1); this is a consequence of isotopic mass balance after the precipitation of ^{30}Si-depleted secondary minerals[79,80]. Groundwaters are also depleted in the light Si isotopes[71] (Figure 1). Modern soils show depletion in ^{30}Si; δ^{30}Si fractionation during adsorption of silica on iron-oxide/hydroxide particles to the extent of ~1.1‰ for ferrihydrite and ~1.6‰ for goethite has been proposed as a possible explanation[76,81]. Lowest δ^{30}Si (–5.7‰) measured in relatively young terrestrial samples is from silcretes (siliceous cements)[34] (Figure 1). Si isotope fractionations have been observed in the siliceous phytoliths of certain land plants and can be explained by silica transport and biomineralization processes[82–84]. In rice plants, both silica concentration as well as δ^{30}Si progressively increase from roots, to stems and leaves and to the husk; rice grains show little silica concentration but very high δ^{30}Si, as high as 6.1‰ (ref. 82). In bamboo trees, silica content increases from stems, through branches to leaves, while δ^{30}Si decreases from roots to stems, but increases from stems through branches to leaves[84] (Figure 1).

Silicon isotopic composition of modern hydrothermal fluids from the East Pacific Rise[85] is similar to that of terrestrial igneous rocks. δ^{30}Si of hydrothermal siliceous precipitates (e.g. from Mariana and Galapagos) shows low values (–0.4‰ to –3.1‰), similar to sinter deposits from continental hot springs[86]. Clearly, amorphous silica precipitates are isotopically lighter than the ambient fluid, although the Si isotope fractionation factor between amorphous silica precipitates and water remains to be determined accurately and could vary as a function of the precipitation mechanism.

The major sink for dissolved silica in the modern oceans is biological uptake, primarily by diatoms as well as radiolaria and sponges. This leads to relatively low silica concentration in the surface waters, which increases to a relatively constant value at greater depths where siliceous skeletons commonly dissolve[85]. The modern ocean is silica-undersaturated with the average concentration of H_4SiO_4 at ~70 μM (2 ppm) (ref. 70). However, silica concentrations show strong lateral and vertical heterogeneity (from <1 to 15 ppm) (refs 70, 87) depending on nutrient availability in surface waters and skeleton dissolution at depth[88]. The residence time of Si in the global oceans is ~15,000 years, although relative to biological uptake from surface waters, it is only ~400 years (ref. 70), implying that Si delivered to the modern oceans is recycled ~40 times through the biological cycle before it departs into a sedimentary sink. Silica secreting organisms preferentially take up lighter Si isotopes with Si isotope fractionation factors ranging from –1.1‰ for diatoms to –3.5‰ in marine sponges[89–91]. Although spatial and depth variation in the sea water δ^{30}Si is well-documented, the mean

δ^{30}Si of modern sea water is estimated at +1.1‰ (ref. 85) (Figure 1), which is higher than the δ^{30}Si of continental and hydrothermal inputs of silicic acid to the oceans. This primarily reflects the preferential uptake of light Si isotopes by silica-secreting organisms in the oceans.

Si isotopes and evolution of sea-water composition through time

Silica-precipitating organisms have played a dominant role in the marine silica cycle throughout the last 550 million years (Ma, Phanerozoic Eon), although the major users of dissolved silica have changed from sponges and radiolaria in the early part of the Phanerozoic to diatoms over the last 200 Ma (refs 92–94). During the Precambrian (older than 550 Ma), silica fluxes into the oceans were likely similar to today, if not higher, given the higher hydrothermal fluxes, inferred from Sr isotopes, in a mantle-buffered Archean ocean (e.g. ref. 95). Silica must continually have left the oceans by means of physiochemical processes, primarily as precipitates during the early stage evaporation of sea water and is preserved primarily as early diagenetic cherts in shallow-water carbonate successions[87,96]. Another significant but more temporally restricted sink for silica are banded iron formations (BIFs). BIFs generally contain 43–56% SiO_2 by weight[97] and as most BIFs, particularly those of Archean age, reflect offshore, commonly basinal deposition, silica precipitation was probably not forced by evaporation of sea water. The recently proposed 'iron shuttle' model[98], involving adsorption of silica on Fe-oxyhydroxides, is a viable mechanism for transporation of silica to deeper parts of the basin and be incorporated into BIFs. Some silica could have been incorporated into clays formed authigenically within sediments (e.g. ref. 99). In the absence of any known biological sink, it is estimated that silica concentration must have been much higher in the Precambrian sea water, perhaps close to amorphous silica saturation[87,94].

Deposits of amorphous silica (now microcrystalline quartz) called cherts (including BIFs) have an ubiquitous presence in the sedimentary rock record. These unique rocks document the evolution of the global silica cycle through geologic time[92,100]. Based on our understanding of modern-day processes, both chert precipitation by evaporation of shallow sea water and clay formation are accompanied by Si isotopic fractionation that leads to enrichment of heavier Si isotopes in ambient sea water. Laboratory experiments have shown that adsorption of silica on Fe-oxyhydroxide particles leads to the progressive enrichment of heavy Si isotopes in the ambient water[81], implying that silica deposition in deeper-water BIFs by the 'iron shuttle' mechanism[98] must also have been accompanied by Si isotope fractionation. Hence, δ^{30}Si of Archean and Proterozoic cherts (Figure 1) can potentially provide insights into the sources and sinks of marine silica before the evolution of silica-precipitating marine organisms like sponges, radiolarians and diatoms in the Phanerozoic. An additional advantage of cherts is their high Si content, which makes them less susceptible to such post-depositional changes and Si isotopes are not thought to be affected by late diagenesis[101].

However, the use of cherts to directly infer the composition of Precambrian sea water has limitations because most of these Precambrian siliceous rocks formed during the diagenesis of precursor sediments, particularly carbonates. This is evident from the preservation of microfossils in Precambrian cherts[102,103]. Several recent studies have reported high-precision MC-ICPMS Si isotope measurements of Archean cherts[31–33,36,37,104–107], while high-precision MC-ICPMS data for Proterozoic cherts are limited[33,108] (Figure 1). Robert and Chaussidon[35] reported *in situ* measurements of the Si isotopic composition of an extensive set of Archean, Proterozoic and some Phanerozoic chert samples using an ion-microprobe technique with a relatively coarse measurement precision (1‰, 2σ) (Figure 1). They interpreted their combined O and Si isotope data from Precambrian cherts to argue for ~70°C paleo-sea-water temperatures, a conclusion that has not received much support[109]. Subsequent studies have highlighted the importance of the source of silica, mechanism of silica precipitation and depositional setting in interpreting the δ^{30}Si of preserved cherts[31,106,107].

δ^{30}Si of Precambrian sea water at any given time can be modeled as a function of δ^{30}Si of continental and hydrothermal inputs and outputs dominated by peritidal chert precipitation and BIF formation, their relative fluxes and the isotopic fractionation factors related to precipitation of silica from sea water or porewater and/or adsorption of silica onto Fe-hydroxide particles during BIF formation. The long residence time of Si relative to ocean mixing timescales indicates that Si in Precambrian cherts was derived from sea water with relatively uniform δ^{30}Si. Hence, δ^{30}Si variations in cherts over time would indirectly reflect the temporal variation of δ^{30}Si of the sea water. A detailed analysis of factors than can cause variation in the sea water δ^{30}Si is presented in Chakrabarti *et al.*[108] and is briefly discussed here.

Although there is marked isotopic variation in δ^{30}Si in cherts from individual Proterozoic basins which can be modelled using Rayleigh-type isotope fractionation[107,108], there is a clear pattern of change in δ^{30}Si from globally distributed cherts throughout the Proterozoic Eon[35,108]. δ^{30}Si increases from 3.8 till 1.5 Ga followed by a decreasing trend which continues into the Phanerozoic (Figure 1). The increasing trend from Archean to Mid-Proterozoic could reflect a gradual change in the dominant silica source from hydrothermal (low δ^{30}Si) to continental (high δ^{30}Si) as well as isotopic fractionation related to precipitation of cherts and BIFs. The highest δ^{30}Si observed in Mid-Proterozoic cherts could reflect an

increase in the δ^{30}Si of the dissolved load in rivers (continental flux) draining into the oceans resulting from increased clay genesis during soil formation as well as interactions of Si with ferric hydroxides in soils after the rise of atmospheric oxygen. The reversal in the above trend towards lower δ^{30}Si since 1.5 Ga is harder to explain based on our knowledge of geological phenomena around that time. In the presence of silica-secreting organisms in the Phanerozoic, the sea water δ^{30}Si and hence that of cherts precipitating from it should have been higher, thereby resulting in an offset in the Proterozoic and Phanerozoic trends. However, this is not observed (Figure 1). The continuum in the Proterozoic and Phanerozoic trends either indicates that silica-secreting marine organisms similar to those found in the Phanerozoic also existed in the Proterozic – a rather unlikely scenario, or that physical mechanisms, similar to the ones discussed above, may be the dominant drivers of the Si isotopic composition of the sea water over time. δ^{30}Si of Phanerozoic cherts[35] are relatively low and overlap with those of diatoms and siliceous sediments from black smokers, suggesting that very little isotopic fractionation has occurred with maturation of these siliceous sediments, although dissolution of diatom silica in sea water, as observed in closed-system experiments, releases fluids with δ^{30}Si lower by ~0.55‰ compared to the starting material[110]. It is clear that temporal variations in δ^{30}Si of cherts cannot be explained solely by simple mixing of isotopically distinct continental and hydrothermal sources unlike other proxies like Nd or Sr isotopes (e.g. refs 111 and 112). The mechanism of silica precipitation and Rayleigh-type fractionation within a single basin also contributes to the variability.

Concluding remarks

The first Si isotope ratio measurements were done over 60 years ago. Early studies involving isotope ratio mass spectrometers (IRMS) investigated broad-scale Si isotope variability in terrestrial and extra-terrestrial samples and were limited by lower-precision and hazardous gases used in sample preparation. Still, important discoveries of large Si isotope fractionations in early-formed Solar System solids, which survived early Solar System processes and are preserved in chondritic meteorites, provided cues to early Solar System evolution. It was also realized that terrestrial igneous rocks do not show much variations in δ^{30}Si. The advent of MC-ICPMS started a new chapter in Si isotope geochemistry. The relative ease of measurements using MC-ICPMS has resulted in wider usage of Si isotopes to investigate natural processes, while considerably improved precision of measurements has helped in understanding a wide range of processes from planetary differentiation, Moon formation, to modern-day surface weathering and modes of silica transport, biological uptake of silica, sea-water compositional variability as well as past sea-water composition. *In situ* Si isotope ratio measurements by laser ablation MC-ICPMS have provided great spatial resolution of sampling without compromising much on the accuracy and precision of the measurements.

1. Halliday, A. N., Applications of multiple collector-ICPMS to cosmochemistry, geochemistry, and paleoceanography. *Geochim. Cosmochim. Acta*, 1998, **62**(6), 919–940.
2. Reviews in Mineralogy and Geochemistry. *Geochemistry of Non-Traditional Stable Isotopes* (eds Johnson, C. M., Beard, B. L. and Albarede, F.), Mineralogical Society of America, 2004, vol. 55.
3. Reynolds, J. H. and Verhoogen, J., Natural variations in the isotopic constitution of silicon. *Geochim. Cosmochim. Acta*, 1953, **3**, 224–234.
4. De La Rocha, C. L., Measurement of silicon stable isotope natural abundances via multicollector inductively coupled plasma mass spectrometry (MC-ICP-MS). *Geochem. Geophys. Geosyst.*, 2002, **3**; doi:10.1029/2002GC000310.
5. Brzezinski, M. A. *et al*., Automated determination of silicon isotope natural abundance by the acid decomposition of cesium hexafluosilicate. *Anal. Chem.*, 2006, **78**, 6109–6114.
6. De La Rocha, C. L., Brzezinski, M. A. and DeNiro, M. J., Purification, recovery, and laser-driven fluorination of silicon from dissolved and particulate silica for the measurement of natural stable isotope abundances. *Anal. Chem.*, 1996, **68**, 3746–3750.
7. Cardinal, D. *et al.*, Isotopic composition of silicon measured by multicollector plasma source mass spectrometry in dry plasma mode. *J. Anal. At. Spectrom.*, 2003, **18**(3), 213–218.
8. Shahar, A. *et al*., Experimentally determined Si isotope fractionation between silicate and Fe metal and implications for Earth's core formation. *Earth Planet. Sci. Lett.*, 2009, **288**(1–2), 228–234.
9. Ziegler, K. *et al*., Metal–silicate silicon isotope fractionation in enstatite meteorites and constraints on Earth's core formation. *Earth Planet. Sci. Lett.*, 2010, **295**, 487–496.
10. Georg, R. B. *et al.*, New sample preparation techniques for the determination of Si isotopic compositions using MC-ICPMS. *Chem. Geol.*, 2006, **235**(1–2), 95–104.
11. Chakrabarti, R. and Jacobsen, S. B., Silicon isotopes in the inner Solar System: Implications for core formation, solar nebular processes and partial melting. *Geochim. Cosmochim. Acta*, 2010, **74**, 6921–6933.
12. Engstrom, E. *et al.*, Chromatographic purification for the determination of dissolved silicon isotopic compositions in natural waters by high-resolution multicollector inductively coupled plasma mass spectrometry. *Anal. Chem.*, 2006, **78**, 250–257.
13. van den Boorn, S. H. J. M. *et al*., Determination of silicon isotope ratios in silicate materials by high-resolution MC-ICP-MS using a sodium hydroxide sample digestion method. *J. Anal. At. Spectrom.*, 2006, **21**(8), 734–742.
14. van den Boorn, S. H. J. M., Vroon, P. Z. and van Bergen, M. J., Sulfur-induced offsets in MC-ICP-MS silicon-isotope measurements. *J. Anal. At. Spectrom.*, 2009, **24**(8), 1111–1114.
15. Weyer, S. and Schwieters, J., High precision Fe isotope measurements with high mass resolution MC-ICPMS. *Int. J. Mass Spectrom.*, 2003, **226**(3), 355–368.
16. Heuser, A. *et al.*, Measurement of calcium isotopes (delta Ca-44) using a multicollector TIMS technique. *Int. J. Mass Spectrom.*, 2002, **220**(3), 385–397.

17. Clayton, R. N., Mayeda, T. K. and Molini-Velsko, C., Isotopic variations in Solar System material: evaporation and condensation of silicates. In *Protostars and Planets II*, University of Arizona Press, 1985, pp. 755–771.
18. Douthitt, C. B., The geochemistry of the stable isotopes of silicon. *Geochim. Cosmochim. Acta*, 1982, **46**(8), 1449–1458.
19. Epstein, S. and Taylor, H. P., 18O/16O, 30Si/28Si, D/H, and 13C/12C studies of lunar rocks and minerals. *Science*, 1970, **167**(3918), 533–535.
20. Epstein, S. and Taylor, H. P., O18/O16, Si30/Si28, D/H, and C13/C12 ratios in lunar samples. In 2nd Lunar Science Conference, Pergamon Press, NY, 1971, pp. 1421–1441.
21. Epstein, S. and Taylor, H. P., O18/O16, Si30/Si28, D/H, and C13/C12 studies of Apollo 14 and 15 samples. In Proceedings of the 3rd Lunar Science Conference 2, Pergamon Press, NY, 1972.
22. Taylor, H. P. and Epstein, S., Oxygen and silicon isotope ratios of lunar-rock-12013. *Earth Planet. Sci. Lett.*, 1970, **9**(2), 208–210.
23. Taylor, H. P. and Epstein, S., Oxygen and silicon isotopes ratios of the Luna 20 soil. *Geochim. Cosmochim. Acta*, 1973, **37**, 1107–1109.
24. Taylor, H. P. and Epstein, S., O18/O16, Si30/Si28 studies of some Apollo 15, 16 and 17 samples. In Proceedings of the 4th Lunar Science Conference, Pergamon Press, NY, 1973.
25. Molini-Velsko, C., Mayeda, T. K. and Clayton, R. N., Isotopic composition of silicon in meteorites. *Geochim. Cosmochim. Acta*, 1986, **50**(12), 2719–2726.
26. Zambardi, T. and Poitrasson, F., Precise determination of silicon isotopes in silicate rock reference materials by MC-ICP-MS. *Geostand. Geoanal. Res.*, 2010, **35**(1), 89–99.
27. Ding, T. *et al.*, Silicon isotope abundance ratios and atomic weights of NBS-28 and other reference materials. *Geochim. Cosmochim. Acta*, 2005, **69**(23), 5487–5494.
28. Reynolds, B. C. *et al.*, An inter-laboratory comparison of Si isotope reference materials. *J. Anal. At. Spectrom.*, 2007, **22**(5), 561–568.
29. Valkiers, S. *et al.*, Silicon isotope amount ratios and molar masses for two silicon isotope reference materials: IRMM-018a and NBS28. *Int. J. Mass Spectrom.*, 2005. **242**(2–3), 319–321.
30. Chmeleff, J. *et al.*, *In situ* determination of precise stable Si isotope ratios by UV-femtosecond laser ablation high-resolution multi-collector ICP-MS. *Chem. Geol.*, 2008, **249**, 155–166.
31. Steinhoefel, G., Horn, I. and Von Blanckenburg, F., Micro-scale tracing of Fe and Si isotope signatures in banded iron formation using femtosecond laser ablation. *Geochim. Cosmochim. Acta*, 2009, **73**, 5343–5360.
32. Steinhoefel, G. *et al.*, Deciphering formation processes of banded iron formations from the Transvaal and the Hamersley successions by combined Si and Fe isotope analysis using UV femtosecond laser ablation. *Geochim. Cosmochim. Acta*, 2010, **74**, 2677–2696.
33. Heck, P. R. *et al.*, SIMS analyses of silicon and oxygen isotope ratios for quartz from Archean and Paleoproterozoic banded iron formations. *Geochim. Cosmochim. Acta*, 2011, **75**, 5879–5891.
34. Basile-Doelsch, I., Meunier, J. D. and Parron, C., Another continental pool in the terrestrial silicon cycle. *Nature*, 2005, **433**(7024), 399–402.
35. Robert, F. and Chaussidon, M., A palaeotemperature curve for the Precambrian oceans based on silicon isotopes in cherts. *Nature*, 2006, **443**(7114), 969–972.
36. Marin-Carbonne, J. *et al.*, A combined *in situ* oxygen, silicon isotopic and fluid inclusion study of a chert sample from Onverwacht Group (3.35 Ga, South Africa): new constraints on fluid circulation. *Chem. Geol.*, 2011, **286**, 59–71.
37. Marin, J., Chaussidon, M. and Robert, F., Microscale oxygen isotope variations in 1.9 Ga Gunflint cherts: assessments of diagenesis effects and implications for oceanic paleotemperature reconstructions. *Geochim. Cosmochim. Acta*, 2010, **74**, 116–130.
38. Clayton, R. N., Mayeda, T. K. and Epstein, S., Isotopic fractionation of silicon in Allende inclusions. In Proceedings of the Lunar Planet Scieince Conference, 1978, pp. 1267–1278.
39. Knight, K. B. *et al.*, Silicon isotopic fractionation of CAI-like vacuum evaporation residues. *Geochim. Cosmochim. Acta*, 2009, **73**(20), 6390–6401.
40. Shahar, A. and Young, E. D., Astrophysics of CAI formation as revealed by silicon isotope LA-MC-ICPMS of an igneous CAI. *Earth Planet. Sci. Lett.*, 2007, **257**, 497–510.
41. Clayton, R. N. *et al.*, Two forsterite-bearing FUN inclusions in the Allende meteorite. *Geochim. Cosmochim. Acta*, 1984, **48**, 535–548.
42. Nittler, L. R. *et al.*, Si and C isotopes in presolar silicon carbide grains from AGB stars. *Nucl. Phys. A*, 2005, **758**, 348c–351c.
43. Timmes, F. X. and Clayton, D. D., Galactic evolution of silicon isotopes: application to presolar SiC grains from meteorites. *Astrophys. J.*, 1996, **472**, 723–741.
44. Georg, R. B. *et al.*, Silicon in the Earth's core. *Nature*, 2007, **447**(7148), 1102–1106.
45. Armytage, R. M. G. *et al.*, Silicon isotopes in meteorites and planetary core formation. *Geochim. Cosmochim. Acta*, 2011, **75**, 3662–3676.
46. Fitoussi, C. *et al.*, Si isotope systematics of meteorites and terrestrial peridotites: implications for Mg/Si fractionation in the solar nebula and for Si in the Earth's core. *Earth Planet. Sci. Lett.*, 2009, **287**(1–2), 77–85.
47. Savage, P. S. and Moynier, F., Silicon isotopic variation in enstatite meteorites: clues to their origin and Earth-forming material. *Earth Planet. Sci. Lett.*, 2013, **361**, 487–496.
48. Fitoussi, C. and Bourdon, B., Silicon isotope evidence against an enstatite chondrite Earth. *Science*, 2012, **335**, 1477–1480.
49. Savage, P. S. *et al.*, Silicon isotope homogeneity in the mantle. *Earth Planet. Sci. Lett.*, 2010, **295**, 139–146.
50. Savage, P. S. *et al.*, Silicon isotope fractionation during magmatic differentiation. *Geochim. Cosmochim. Acta*, 2011, **75**, 6124–6139.
51. Birch, F., Elasticity and constitution of the Earth interior. *J. Geophys. Res.*, 1952, **57**(2), 227–286.
52. Birch, F., Density and composition of mantle and core. *J. Geophys. Res.*, 1964, **69**(20), 4377–4388.
53. Poirier, J.-P., Light elements in the Earth's outer core: a critical review. *Phys. Earth Planet. Inter.*, 1994, **85**, 319–337.
54. Li, J. and Fei, Y., Experimental constriants on core composition. In *Treatise on Geochemistry* (ed. Carlson, R. W.), 2004, pp. 521–546.
55. Shahar, A. *et al.*, High-temperature Si isotope fractionation between iron metal and silicate. *Geochim. Cosmochim. Acta*, 2011, **75**, 7688–7697.
56. Schauble, E. A. *et al.*, Estimating magnesium and silicon isotope fractionation with first-principles lattice dynamics. *Geochim. Cosmochim. Acta*, 2007, **71**(15), A884.
57. Corgne, A. *et al.*, Metal–silicate partitioning and constraints on core composition and oxygen fugacity during Earth accretion. *Geochim. Cosmochim. Acta*, 2008, **72**(2), 574–589.
58. Gessmann, C. K. and Rubie, D. C., The origin of the depletions of V, Cr and Mn in the mantles of the Earth and Moon. *Earth Planet. Sci. Lett.*, 2000, **184**(1), 95–107.
59. Gessmann, C. K. *et al.*, Solubility of silicon in liquid metal at high pressure: implications for the composition of the Earth's core. *Earth Planet. Sci. Lett.*, 2001, **184**(2), 367–376.
60. Kilburn, M. R. and Wood, B. J., Metal–silicate partitioning and the incompatibility of S and Si during core formation. *Earth Planet. Sci. Lett.*, 1997, **152**(1–4), 139–148.
61. Wiechert, U. and Halliday, A. N., Oxygen isotopes and the Moon-forming giant impact. *Science*, 2001, **294**, 345–348.

62. Lugmair, G. W. and Shukolyukov, A., Early solar system timescales according to ^{53}Mn–^{53}Cr systematics. *Geochim. Cosmochim. Acta*, 1998, **62**(16), 2863–2886.
63. Touboul, M. *et al*., Late formation and prolonged differentiation of the Moon inferred from W isotopes in lunar metals. *Nature*, 2007, **450**, 1206–1209.
64. Trinquier, A. *et al.*, Origin of nucleosynthetic isotope heterogeneity in the solar protoplanetary disk. *Science*, 2009, **324**, 374–376.
65. Canup, R. M. and Asphaug, E., Origin of the Moon in a giant impact near the end of the Earth's formation. *Nature*, 2001, **412**(6848), 708–712.
66. Pahlevan, K. and Stevenson, D. J., Equilibration in the aftermath of the lunar-forming giant impact. *Earth Planet. Sci. Lett.*, 2007, **262**(3–4), 438–449.
67. Pahlevan, K., Stevenson, D. J. and Eiler, J. M., Chemical fractionation in the silicate vapor atmosphere of the Earth. *Earth Planet. Sci. Lett.*, 2011, **301**, 433–443.
68. Armytage, R. M. G. *et al*., Silicon isotopes in lunar rocks: implications for the Moon's formation and the early history of the Earth. *Geochim. Cosmochim. Acta*, 2012, **77**, 504–514.
69. Cuk, M. and Stewart, S. T., Making the Moon from a fast-spinning Earth: a giant impact followed by resonant despinning. *Science*, 2012, **338**, 1047–1052.
70. Treguer, P. *et al.*, The silica balance in the World Ocean – a reestimate. *Science*, 1995, **268**, 375–379.
71. Georg, R. B. *et al.*, Silicon fluxes and isotope composition of direct groundwater discharge into the Bay of Bengal and the effect on the global ocean silicon isotope budget. *Earth Planet. Sci. Lett.*, 2009, **283**(1–4), 67–74.
72. Bern, C. R. *et al*., Weathering, dust, and biocycling effects on soil silicon isotope ratios. *Geochim. Cosmochim. Acta*, 2010, **74**, 876–889.
73. Cornelis, J. T. *et al*., Tracing mechanisms controlling the release of dissolved silicon in forest soil solutions using Si isotopes and Ge/Si ratios. *Geochim. Cosmochim. Acta*, 2010, **74**, 3913–3924.
74. Georg, R. B. *et al.*, Silicon isotope variations accompanying basalt weathering in Iceland. *Earth Planet. Sci. Lett.*, 2007, **261**(3–4), 476–490.
75. Opfergelt, S. *et al.*, Variations of δ^{30}Si and Ge/Si with weathering and biogenic input in tropical basaltic ash soils under monoculture. *Geochim. Cosmochim. Acta*, 2010, **74**, 225–240.
76. Opfergelt, S. *et al.*, Impact of soil weathering degree on silicon isotopic fractionation during adsorption onto iron oxides in basaltic ash soils, Cameroon. *Geochim. Cosmochim. Acta*, 2009, **73**(24), 7226–7240.
77. Ziegler, K. *et al*., Natural variations of delta Si-30 ratios during progressive basalt weathering, Hawaiian Islands. *Geochim. Cosmochim. Acta*, 2005, **69**(19), 4597–4610.
78. Meheut, M. *et al.*, Equilibrium isotopic fractionation in the kaolinite, quartz, water system: prediction from first-principles density-functional theory. *Geochim. Cosmochim. Acta*, 2007, **71**, 3170–3181.
79. Ding, T. *et al*., Silicon isotope compositions of dissolved silicon and suspended matter in the Yangtze River, China. *Geochim. Cosmochim. Acta*, 2004, **68**(2), 205–216.
80. Georg, R. B. *et al*., Mechanisms controlling the silicon isotopic compositions of river waters. *Earth Planet. Sci. Lett.*, 2006, **249**(3–4), 290–306.
81. Delstanche, S. *et al.*, Silicon isotopic fractionation during adsorption of aqueous monosilicic acid onto iron oxide. *Geochim. Cosmochim. Acta*, 2009, **73**(4), 923–934.
82. Ding, T. P. *et al.*, Silicon isotope study on rice plants from the Zhejiang province, China. *Chem. Geol.*, 2005, **218**(1–2), 41–50.
83. Ding, T. P. *et al*., Silicon isotope fractionation between rice plants and nutrient solution and its significance to the study of the silicon cycle. *Geochim. Cosmochim. Acta*, 2008, **72**(23), 5600–5615.
84. Ding, T. P. *et al*., Silicon isotope fractionation in bamboo and its significance to the biogeochemical cycle of silicon. *Geochim. Cosmochim. Acta*, 2008, **72**(5), 1381–1395.
85. De La Rocha, C. L., Brzezinski, M. A. and DeNiro, M. J., A first look at the distribution of the stable isotopes of silicon in natural waters. *Geochim. Cosmochim. Acta*, 2000, **64**(14), 2467–2477.
86. Ding, T. *et al*., *Silicon Isotope Geochemistry*, Geological Publishing House, Beijing, China, 1996.
87. Siever, R., The silica cycle in the precambrian. *Geochim. Cosmochim. Acta*, 1992, **56**(8), 3265–3272.
88. Reynolds, B. C., Jaccard, S. L. and Haliday, A. N., Abrupt cessation of North Pacific upwelling with northern hemisphere glaciation recorded by silicon isotopes. *Geochim. Cosmochim. Acta*, 2006, **70**, A530.
89. Beucher, C. P., Brzezinski, M. A. and Jones, J. L., Sources and biological fractionation of Silicon isotopes in the Eastern Equatorial Pacific. *Geochim. Cosmochim. Acta*, 2008, **72**, 3063–3073.
90. De La Rocha, C. L., Silicon isotope fractionation by marine sponges and the reconstruction of the silicon isotope composition of ancient deep water. *Geology*, 2003, **31**(5), 423–426.
91. De La Rocha, C. L., Brzezinski, M. A. and DeNiro, M. J., Fractionation of silicon isotopes by marine diatoms during biogenic silica formation. *Geochim. Cosmochim. Acta*, 1997, **61**(23), 5051–5056.
92. Maliva, R. G., Knoll, A. H. and Siever, R., Secular change in chert distribution: a reflection of evolving biological participation in the silica cycle. *Palaios*, 1989, **4**, 519–532.
93. Maliva, R. G. and Siever, R., Chertification histories of some Late Mesozoic and Middle Paleozoic platform carbonates. *Sedimentology*, 1989, **36**, 907–926.
94. Siever, R., Silica in the oceans: biological–geochemical interplay. In *Scientists on Gaia* (eds Schneider, S. and Boston, P. J.), MIT Press, 1991, pp. 287–295.
95. Shields, G. and Veizer, J., Precambrian marine carbonate isotope database: version 1.1. *Geochem. Geophys. Geosyst.*, 2002, **3**; doi:10.1029/2001GC000266.
96. Knauth, L. P., A model for the origin of chert in limestone. *Geology*, 1979, **7**, 274–277.
97. Klein, C., Some Precambrian banded iron-formations (BIFs) from around the world: their age, geologic setting, mineralogy, metamorphism, geochemistry, and origin. *Am. Mineral.*, 2005, **90**, 1473–1499.
98. Fischer, W. W. and Knoll, A. H., An iron shuttle for deepwater silica in Late Archean and early Paleoproterozoic iron formation. *Geol. Soc. Am. Bull.*, 2009, **121**(1–2), 222–235.
99. Tosca, N. J. *et al*., Clay mineralogy, organic carbon burial, and redox evolution in Proterozoic oceans. *Geochim. Cosmochim. Acta*, 2010, **74**, 1579–1592.
100. Maliva, R. G., Knoll, A. H. and Simonson, B. M., Secular change in the Precambrian silica cycle: insights from chert petrology. *Geol. Soc. Am. Bull.*, 2005, **117**(7–8), 835–845.
101. Posth, N. R. *et al*., Alternating Si and Fe deposition caused by temperature fluctuations in Precambrian oceans. *Nature Geosci.*, 2008, **1**, 703–708.
102. Barghoorn, E. S. and Tyler, S. A., Microorganisms from the Gunflint chert. *Science*, 1965, **147**, 563–577.
103. Knoll, A. H., Exceptional preservation of photosynthetic organisms in silicifed carbonates and silicified peats. *Philos. Trans. R. Soc. London*, 1985, **311**, 111–122.
104. Abraham, K. *et al*., Coupled silicon–oxygen isotope fractionation traces Archaean silicification. *Earth Planet. Sci. Lett.*, 2011, **301**, 222–230.

105. Andre, L. *et al*., Silicon isotopes in 3.8 Ga West Greenland rocks as clues to the Eoarchaean supracrustal Si cycle. *Earth Planet. Sci. Lett.*, 2006, **245**(1–2), 162–173.
106. van den Boorn, S. H. J. M. *et al*., Dual role of seawater and hydrothermal fluids in Early Archean chert formation: evidence from silicon isotopes. *Geology*, 2007, **35**(10), 939–942.
107. van den Boorn, S. H. J. M. *et al.*, Silicon isotope and trace element constraints on the origin of ~3.5 Ga cherts: implications for Earth Archaean marine environments. *Geochim. Cosmochim. Acta*, 2010, **74**, 1077–1103.
108. Chakrabarti, R. *et al.*, Si isotope variability in Proterozoic cherts. *Geochim. Cosmochim. Acta*, 2012, **91**, 187–201.
109. Blake, R. E., Chang, S. J. and Lepland, A., Phopshate oxygen isotope evidence for a temperate and biologically active Archean ocean. *Nature*, 2010, **464**, 1029–1232.
110. Demarest, M. S., Brzezinski, M. A. and Beucher, C. P., Fractionation of silicon isotopes during biogenic silica dissolution. *Geochim. Cosmochim. Acta*, 2009, **73**, 5572–5583.
111. Asmerom, Y. *et al.*, Strontium isotopic variations of Neoproterozoic seawater – implications for crustal evolution. *Geochim. Cosmochim. Acta*, 1991, **55**, 2883–2894.
112. Derry, L. A. and Jacobsen, S. B., The chemical evolution of Precambrian seawater – evidence from REEs in banded iron formations. *Geochim. Cosmochim. Acta*, 1990, **54**, 2965–2977.

Received 14 November 2014; accepted 29 December 2014